The Initial Mass Function

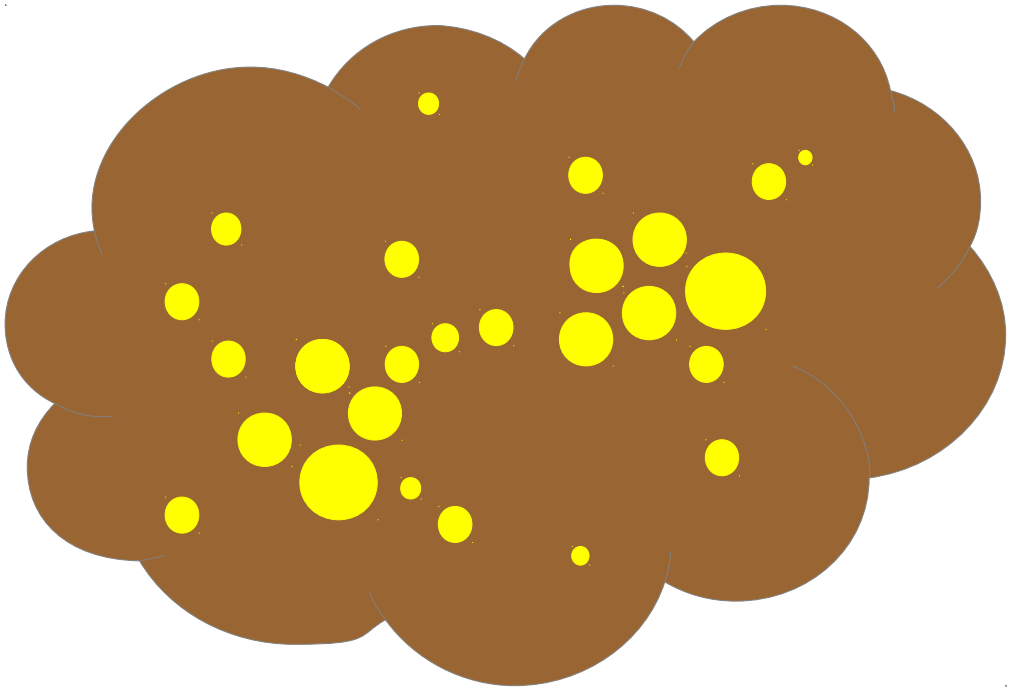

Elisa Chisari

AST 541
Dec 4 2012

Outline

The form of the IMF
Summary of observations
Ingredients of a complete model
A Press-Schechter model
Numerical simulations
Conclusions

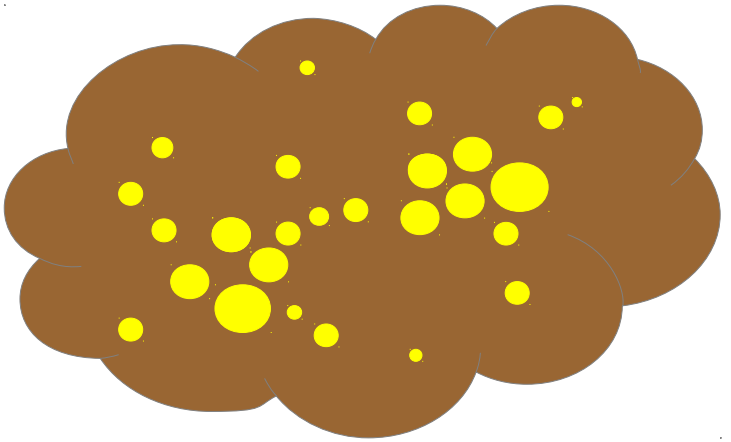

The form of the IMF

Bastian et al. (2010)

IMF: the number of stars per mass (or log-mass) bin

$$\Phi(logm) = dN/d\log m \propto m^{-\Gamma}, \quad \textbf{or}$$
$$\chi(m) = dN/dm \propto m^{-\alpha}, \quad \textbf{with} \quad \alpha = 1+\Gamma$$

Salpeter (1955), single power-law

Example: Kroupa IMF, segmented

$$dN \propto m^{-2.3} dm \quad (m \geq 0.5 M_\odot)$$
$$dN \propto m^{-1.3} dm \quad (0.08 \leq m \leq 0.5 M_\odot)$$
$$dN \propto m^{-0.3} dm \quad (m \leq 0.08 M_\odot).$$

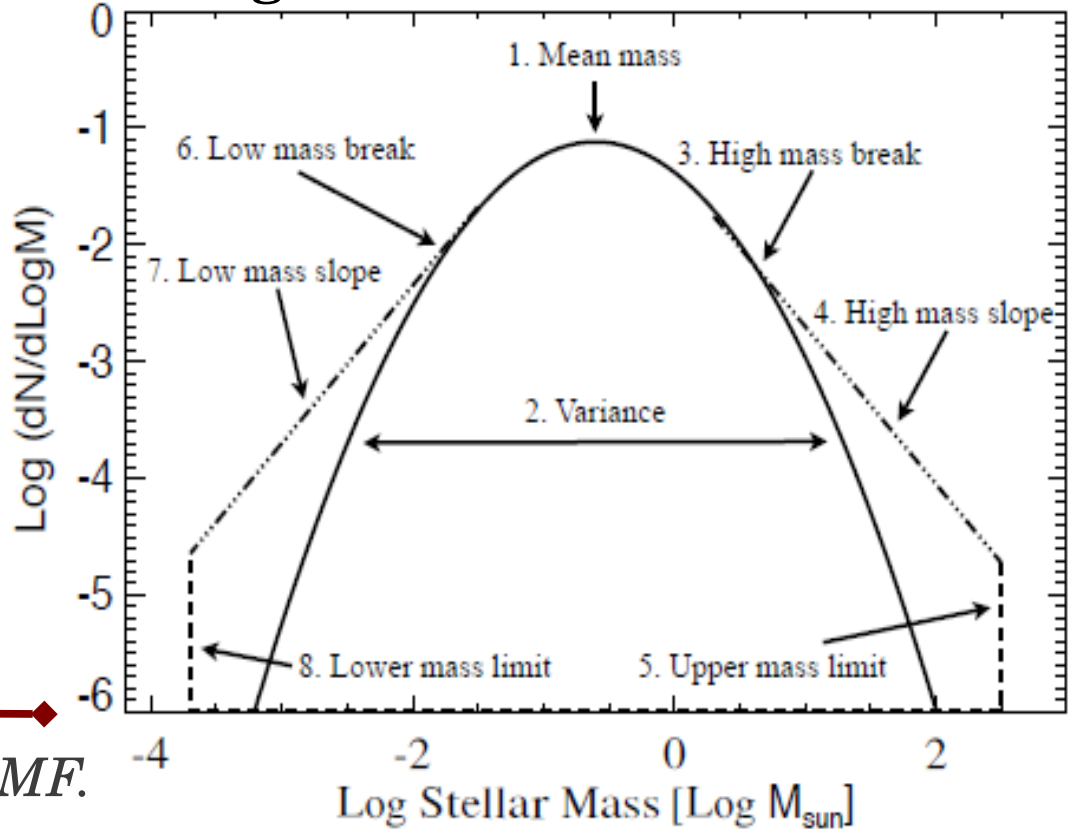

NB: It is not sufficient to reproduce the IMF.

"A non-exhaustive list also includes the **star formation rate and efficiency, the structure and kinematics of stellar groups and clusters, the properties of multiple stellar systems, jets, and protoplanetary discs, and the rotation rates of stars**. (...) variations in **environment and initial conditions**." **Bate (2012)**

Observations

The measured PDMF and inferred IMF

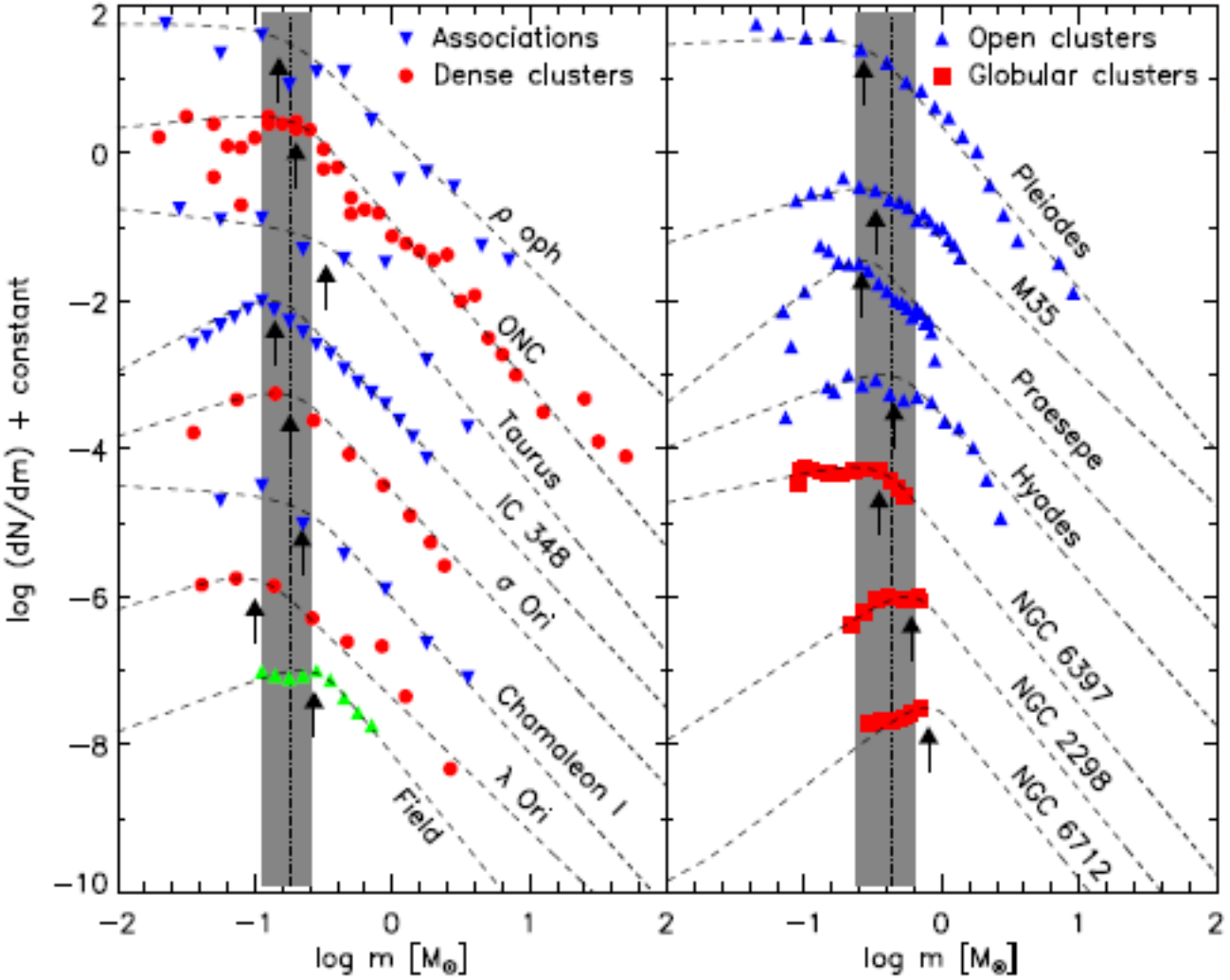

$$\chi(m) = \frac{dN}{dm} \propto m^{-\alpha}[1 - e^{(-m/m_p)^{\beta}}]$$

in Bastian et al. (2010), from de Marchi et al. (2010)

Observations

Bastian et al. (2010)

Difficulties in determining IMF

- Assumed **spatially constant**. Field and cluster population differ in the high-mass stars.
- **PDMF** vs. IMF: Assumes IMF is **constant in time** and knowledge of **SFH**.
- In clusters, **PDMF** changed by **dynamics.**
- **Sub-stellar** objects ambiguities: mass-luminosity evolves strongly with time, difficult to infer **mass/age.**
- **Multiplicity fraction:** the IMF is sensitive to it through the binary (multiple) fraction and the mass ratio (missing detections unresolved secondaries (companions) in the luminosity function). Assumes these are **constant in time.**

  E.g., high mass ratio systems can "*hide*" stars

*And we need to be careful about the **statistics** of the IMF*

Observations

The core mass function (CMF)

Pipe nebula (130pc, 10^4 solar mass)

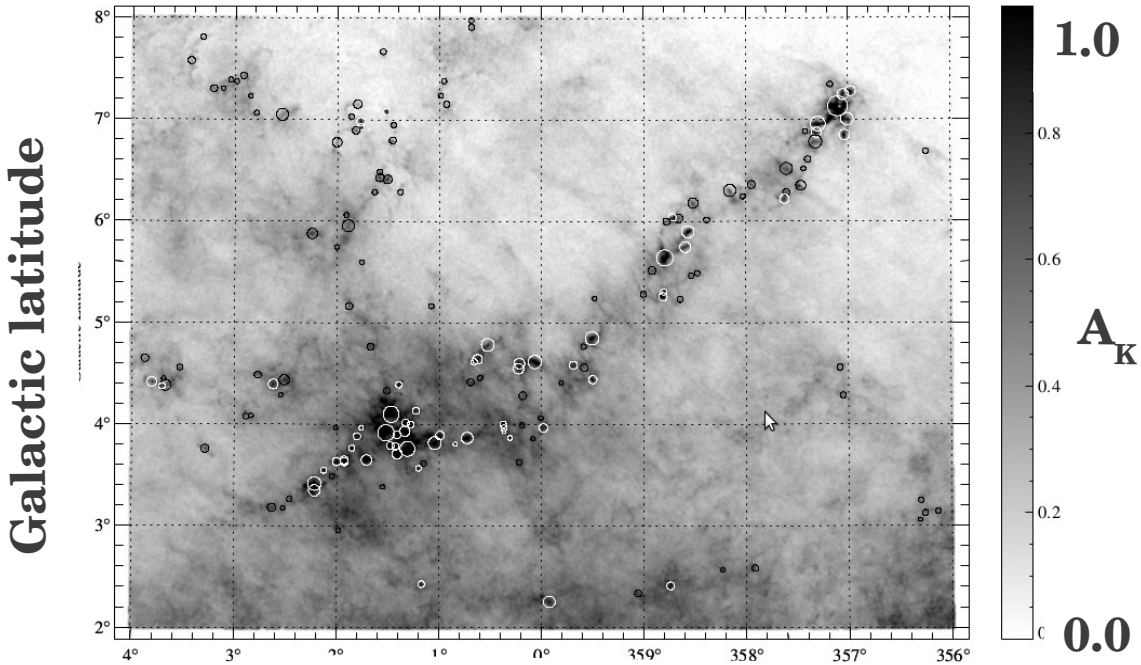

6 deg x 8 deg Galactic longitude

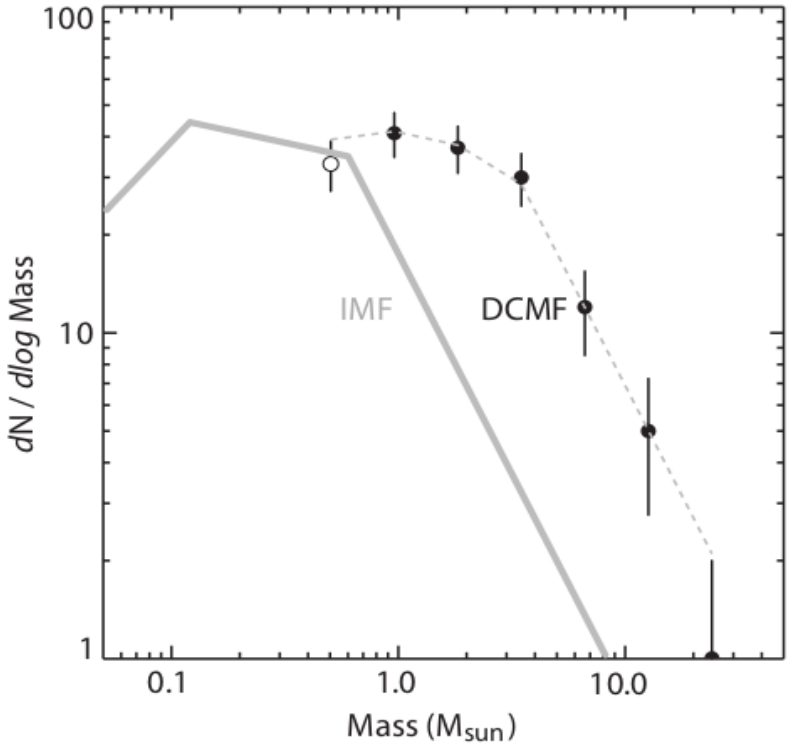

Fig. 2. Mass function of dense molecular cores plotted as filled circles with error bars. The grey line is the stellar IMF for the Trapezium cluster (Muench et al. 2002). The dashed grey line represents the stellar IMF in binned form matching the resolution of the data and shifted to higher masses by about a factor of 4. The dense core mass function is similar in shape to the stellar IMF function, apart from a uniform star formation efficiency factor.

Extinction maps from 4 million background stars in the IR (2MASS) provide high contrast to identify the cores (~160) in $C^{18}O, H^{13}CO^+$

Lombardi et al. (2006), Alves et al. (2007)

Towards a complete model of the IMF

... or the AST541 summary of Star Formation

Physical processes that determine the IMF

- Gravitational collapse and fragmentation (Andrea/Mary Anne)
- Turbulence (Sasha)
- Accretion (Wendy, Sudhir)
- Magnetic Fields (Emmanuel)
- Feedback (Ai-Lei)
- Stellar interactions (Alex)
- Environment (Colin)

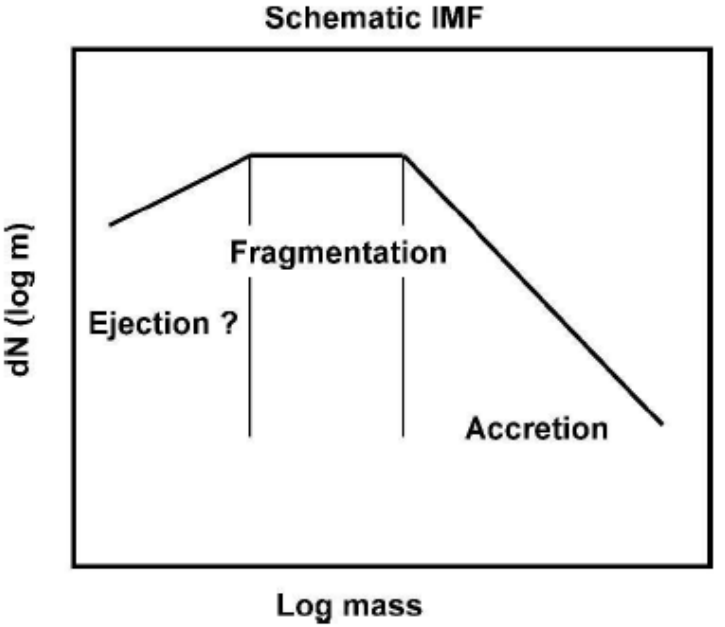

Fig. 11.— A schematic IMF showing the regions that are expected to be due to the individual processes. The peak of the IMF and the characteristic stellar mass are believed to be due to gravitational fragmentation, while lower mass stars are best understood as being due to fragmentation plus ejection or truncated accretion while higher-mass stars are understood as being due to accretion.

Bonnell et al. (2007)

Towards a complete model of the IMF

ANALYTIC APPROACH

Central Limit Theorem
The sum of an infinite number of independent variables:

$$\log m = \Sigma_i \log y_i$$

$$\rightarrow \quad \varphi(m) \sim e^{\frac{-(\log m - \log m_c)^2}{2\sigma^2}}$$

Press-Schechter theory

Commonly used in cosmology. Well-understood, but cannot capture many of the physical mechanisms in simulations.

Press-Schechter (1974)

NUMERICAL SIMULATIONS

Adaptive Mesh Refinement (AMR)

Increased resolution in denser regions. Magnetic fields, radiation transport and shocks.

Smoothed Particle Hydrodynamics (SPH)

Particles + smoothing kernel → fluid
Suitable for self-gravitating fluids and incorporating turbulence. No need for refinement because you follow particles. But requires **artificial viscosities** to make particles behave more like fluid and for shock discontinuities.

Press-Schechter model

Original formalism by **Press-Schechter (1974)**, applied to the halo mass function in cosmological context.

The ingredients

$\delta = \rho/\bar{\rho} - 1$

$$\mathcal{P}(\delta) = \frac{1}{\sqrt{2\pi\sigma^2}} \exp\left(-\frac{\delta^2}{2\sigma^2}\right) \qquad \sigma^2(R) = \int_0^\infty \tilde{\delta}^2(k) W_k^2(R) d^3k,$$

+ *density threshold for star formation*

Star formation: thermal pressure, turbulence, magnetic fields prevent collapse

$$\mathcal{P}(\delta) = \frac{1}{\sqrt{2\pi\sigma_0^2}} \exp\left(-\frac{(\delta-\bar{\delta})^2}{2\sigma_0^2}\right)$$

$\delta = \log(\rho/\bar{\rho})$

$$\sigma_0^2 = \ln(1 + b\mathcal{M}^2)$$

Mach number

$b \simeq 0.25$

$$\sigma^2(R) = \int_{2\pi/L_i}^{\infty} \tilde{\delta}^2(k) W_k^2(R)\, d^3k = \int_{2\pi/L_i}^{2\pi/R} \tilde{\delta}^2(k) 4\pi k^2 dk = C\left(1 - \left(\frac{R}{L_i}\right)^{n'-3}\right)$$

Cut-off at large scales

$n' \sim 11/3$

$$\mathcal{P}_R(\delta) = \frac{1}{\sqrt{2\pi\sigma(R)^2}} \exp\left(-\frac{(\delta + \frac{\sigma(R)^2}{2})^2}{2\sigma(R)^2}\right)$$

Hennebelle & Chabrier (2008)

Press-Schechter model

$$\mathcal{P}_R(\delta) = \frac{1}{\sqrt{2\pi\sigma(R)^2}} \exp\left(-\frac{(\delta + \frac{\sigma(R)^2}{2})^2}{2\sigma(R)^2}\right)$$

Hennebelle & Chabrier (2008)

Thermal pressure: Jeans mass $\delta \geq -2\ln\left(M/M_J^0\right)$ OR $\delta \geq \delta_R^c = -2\ln\left(\frac{R}{\lambda_J^0}\right)$

Unlike in cosmology, the threshold depends on R

Turbulent support: modification to Jeans mass

$$\langle V_{\rm rms}^2 \rangle = V_0^2 \times \left(\frac{R}{1{\rm pc}}\right)^{2\eta} \quad \rightarrow \quad \eta = \frac{n-3}{2}$$

Connection between Larson index and Kolmogorov turbulence

with $V_0 \simeq 1$ km s^{-1} and $\eta \simeq 0.4$-0.5 (Larson 1981)

$$M \geq M_R^c = a_J^{2/3} \frac{V_0^2}{3G} \left(\frac{R}{1{\rm pc}}\right)^{2\eta} R$$

$$\delta \geq \delta_R^c = \ln\left[\frac{a_J^{2/3}}{3} \frac{V_0^2}{G\bar{\rho}R^2} \left(\frac{R}{1{\rm pc}}\right)^{2\eta}\right]$$

Magnetic field:

$B \propto \rho^{1/2}\Delta V$ **(NS)**

1) $a_J \times [1 + (V_A^0/C_s)^2/6]^{3/2}$
2) **Changes Mach number and PDF**

Press-Schechter model

DERIVATION of the IMF form

Hennebelle & Chabrier (2008)

Mass contained in structures of mass with $M < M_R^c$

(1) $$M_{\rm tot}(R) = L_i^3 \int_{\delta_R^c}^{\infty} \bar{\rho} \exp(\delta) \mathcal{P}_R(\delta) d\delta.$$

(2) $$M_{\rm tot}(R) = L_i^3 \int_0^{M_R^c} M' \mathcal{N}(M') P(R, M') dM'.$$

Jeans unstable clouds are embedded in bigger Jeans unstable clouds.

$P(R, M') = 1$

(1) = (2) →

$$\mathcal{N}(M_R^c) = \frac{\bar{\rho}}{M_R^c} \frac{dR}{dM_R^c} \left(-\frac{d\delta_R^c}{dR} \exp(\delta_R^c) \mathcal{P}_R(\delta_R^c) + \int_{\delta_R^c}^{\infty} \exp(\delta) \frac{d\mathcal{P}_R}{dR} d\delta \right)$$

IGNORED

PROBLEMS: velocity-density correlations, time dependence, accretion/merging, fragmentation

significant when $R \simeq L_i$
size structure ~ system

Press-Schechter model

Hennebelle & Chabrier (2008)

Thermal support

$$\mathcal{N}(\widetilde{M}) \simeq \frac{2\bar{\rho}}{(M_J^0)^2}\,\widetilde{M}^{-3-\frac{2\ln(\widetilde{M})}{\sigma^2}} \times \frac{\exp(-\sigma^2/8)}{\sqrt{2\pi}\,\sigma}$$

$$\widetilde{M}_\sigma^{\pm} = \exp(\pm\frac{3}{2}\sigma^2)$$

$$\widetilde{M}_\sigma^{\pm} = (1+b\mathcal{M}^2)^{\pm\frac{3}{2}}$$

where $\widetilde{M} = M/M_J^0$.

2 REGIMES

Lognormal	*power-law*	
$M_\sigma^- \ll \widetilde{M} \ll M_\sigma^+$	$M \gg M_\sigma^+$ $M \ll M_\sigma^-$	$n=-3$

Purely thermal, much steeper than Salpeter slope.

Turbulent support: increases with scale

$$\mathcal{N}(\widetilde{M}) = \frac{2\bar{\rho}}{(M_J^0)^2}\,\frac{(1-\eta)}{(2\eta+1)}\,\mathcal{M}_*^{6/(\eta-1)}\,\widetilde{M}'^{-3\alpha_1-\frac{2(\alpha_2)^2}{\sigma^2}\ln(\widetilde{M}')} \times \frac{\exp(-\sigma^2/8)}{\sqrt{2\pi}\,\sigma},$$

where $\widetilde{M} = M/M_J^0$, $\widetilde{M}' = \mathcal{M}_*^{3/(\eta-1)}\widetilde{M}$, $\alpha_1 = (1+\eta)/(2\eta+1)$, $\alpha_2 = (\eta-1)/(2\eta+1)$, $\alpha_3 = 6/(2\eta+1)$, and

$$\mathcal{M}_* = \frac{1}{\sqrt{3}}\frac{V_0}{C_s}\left(\frac{\lambda_J^0}{1\mathrm{pc}}\right)^{\eta}$$

$\eta \simeq 0.4$
$n \simeq 2.33$

Purely turbulent, reproduces Salpeter slope.

Press-Schechter model

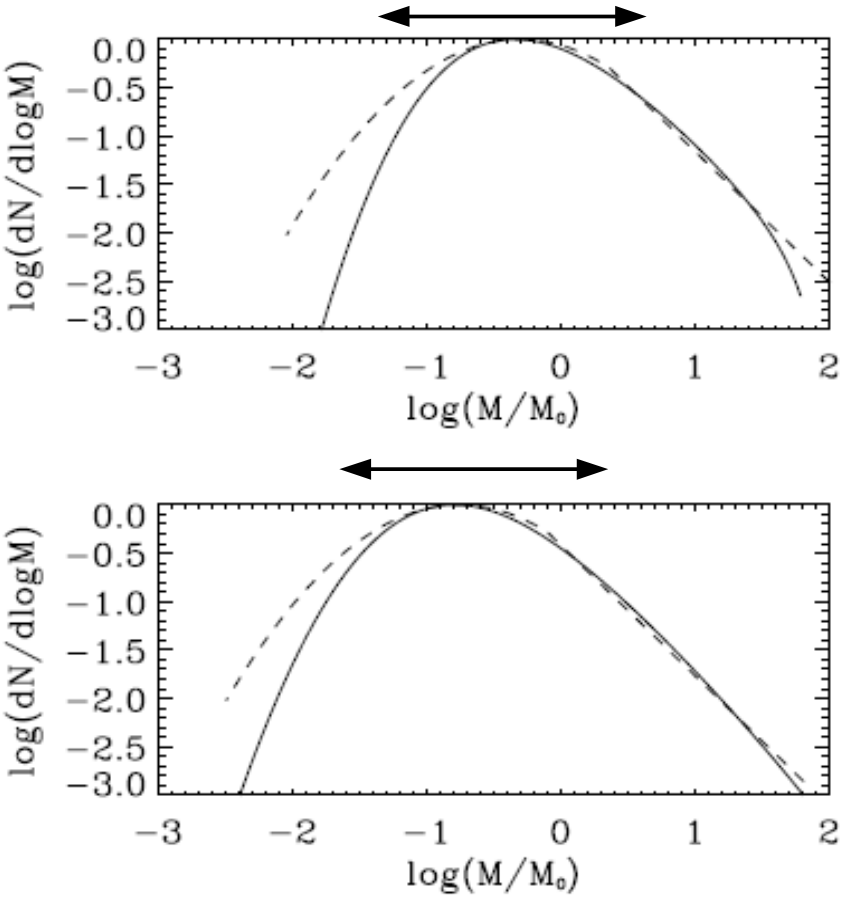

Hennebelle & Chabrier (2008)

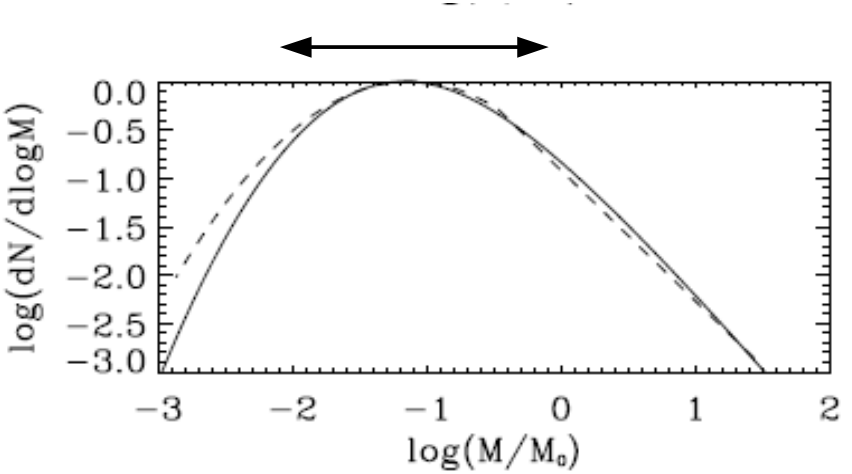

FIG. 5.— Comparison between the theoretical IMF/CMF, $dN/d\log M$ (*solid line*), obtained with $\mathcal{M} = 6$ (*top*), 12 (*middle*), 25 (*bottom*), and $\mathcal{M}_*^2 = 2$ and the stellar/brown dwarf *system* IMF (*dotted line*) of Chabrier (2003a). The peak of this latter IMF has been adjusted arbitrarily to the one of each theoretical mass function.

Thermal support **Turbulent support: increases with scale**

Transition $\widetilde{M}_\sigma^{\pm} = (1 + b\mathcal{M}^2)^{\pm\frac{3}{2}}$. $\widetilde{M}^* \simeq 2(\mathcal{M}_*)^{-1/\eta}$.

Peak $\widetilde{M}_{\rm peak} = \exp(-\frac{3}{4}\sigma^2) = \frac{1}{(1 + b\mathcal{M}^2)^{3/4}}$.

Numerical simulations

AMR radiative-hydro simulations of star cluster formation

Krumholz et al. (2012)

ORION: radiative transfer, hydrodynamics, self-gravity, accreting sink particles, a model for protostellar evolution and feedback which includes **stellar radiation and outflows.**

Initial conditions

$M_c = 1000 M_{Sun}$ $\sigma_c = 2.9\ km/s$

$\Sigma_c = 1\ g/cm^2$ $T_g = 10K$

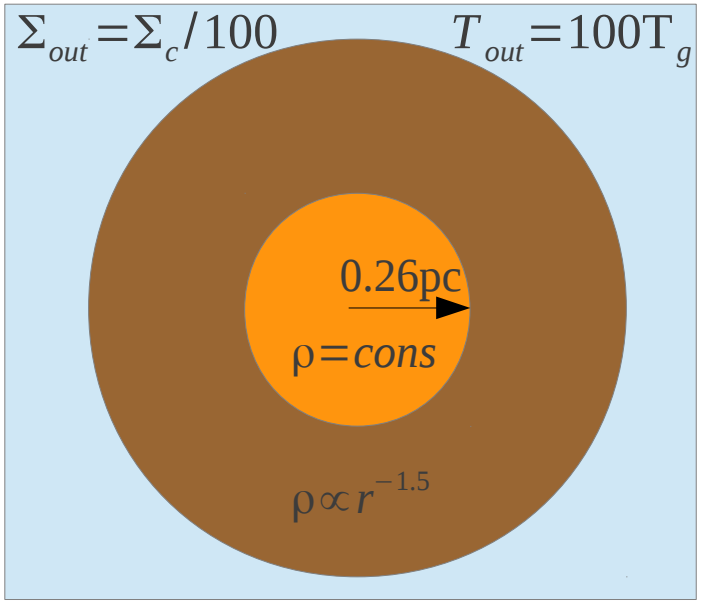

3 cases

- **Smooth, no winds**
- **Turbulent, no winds**
- **Turbulent, with winds**

Turbulent initial conditions

Evolve for 2 crossing times, no gravity, no feedback, isothermal.

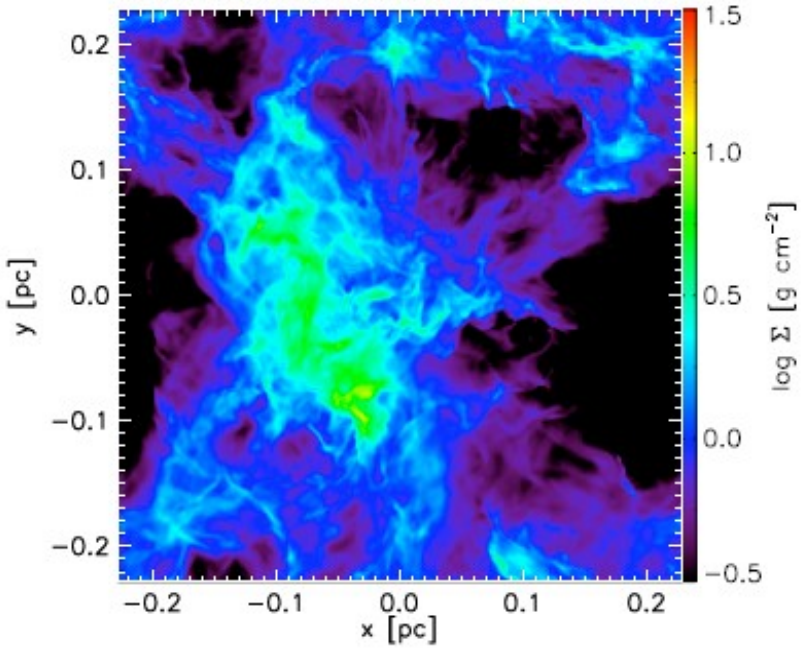

Numerical simulations

AMR radiative-hydro simulations of star cluster formation

Conditions for refinement:

- **Density exceeds local Jeans density**
- **Sharp radiation energy gradient**
- **Proximity to star particle**

Maximum refinement

Smooth, no winds: 40AU

Turbulent: 23AU

Krumholz et al. (2012)

Star particles when M>0.05 solar mass

Smooth, no winds

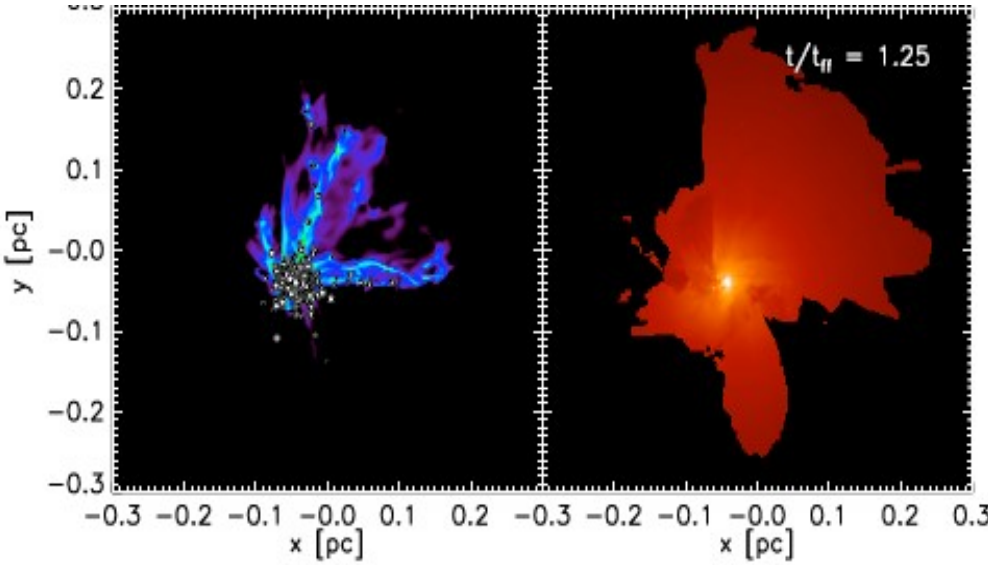

$\log \Sigma \simeq 0.3 - 30 \mathrm{g}/cm^2$

Turbulent, with winds

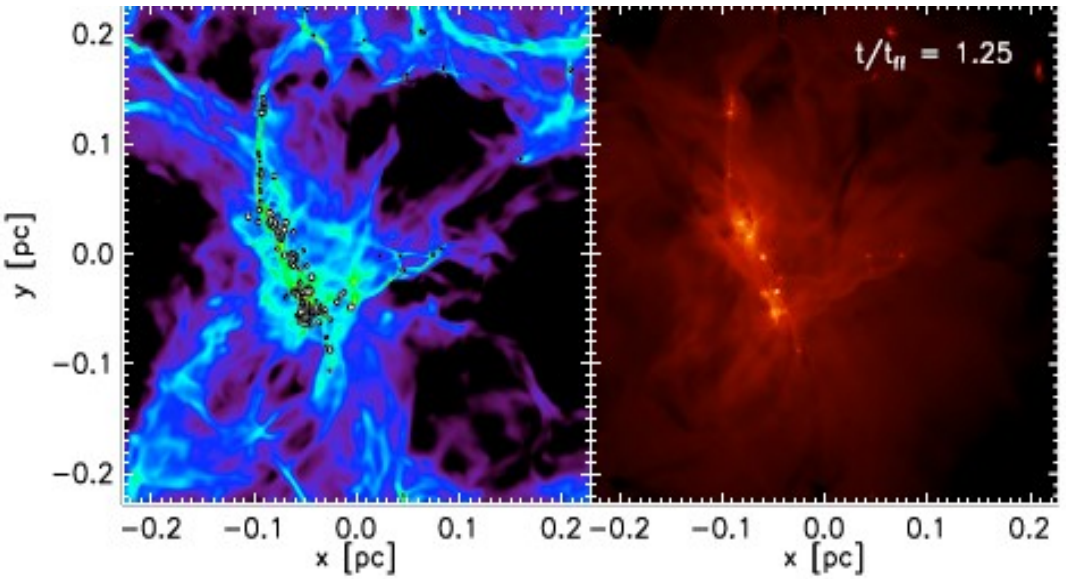

$\log T \simeq 0 - 100\mathrm{K}$

Radiation feedback vs outflows: RF prevents brown dwarfs and allows massive stars. Too efficient! Outflows needed to avoid too much accretion luminosity.

Numerical simulations

AMR radiative-hydro simulations of star cluster formation

Krumholz et al. (2012)

- **SmNW** starts off more **slowly** than Tu case, where SFR is constant and low.
- **SmNW** has too much **accretion luminosity,** no new stars are formed and the ones present continue growing, this displaces the **IMF to larger masses**. The gas is at **higher T** than in Tu case. Incorporating outflows has produced hypothesized result.

Tu: 10% mass in stars

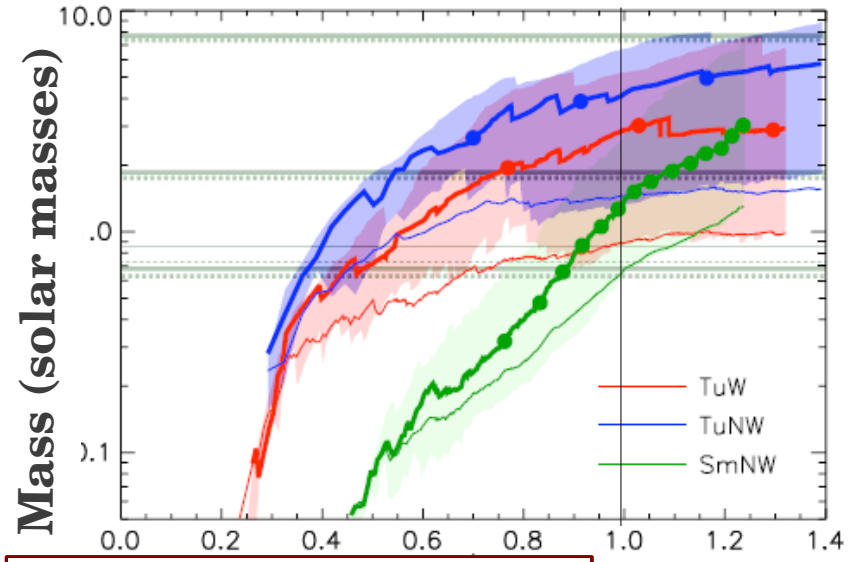

$$\sum_{m_* < M_n} m_* = \frac{n}{100} \sum m_*$$

$t_{ff} = (3\pi/32 G \bar{\rho}_M(0))^{1/2}$

56 Sm/23 Tu kyr

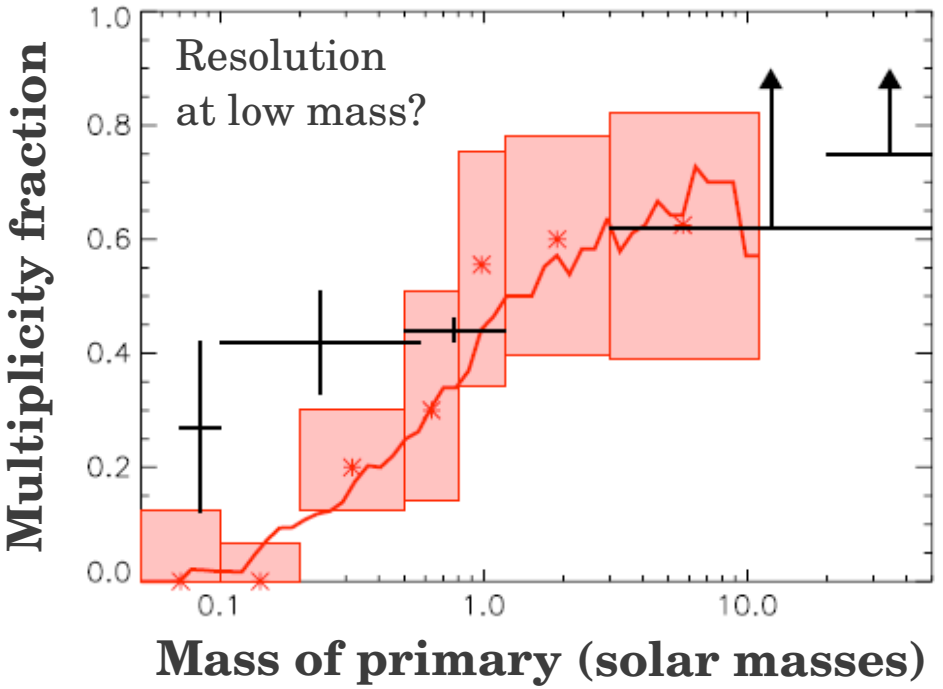

Numerical simulations

SPH radiative-hydro simulations of star cluster formation

Bate (2012)

Initial conditions

Turbulent velocity field
consistent with Larson relation

$M_c = 500 M_{Sun}$ $T_g = 10.3 K$

$\rho_c = 1.2 \times 10^{-19} g/cm^3$ $Rc = 0.404 pc$

3.5×10^7 particles $t_{ff} = 19 kyr$

Sink particles $r_{acc} = 0.5 AU$ **<< 23AU**
neglect radiative feedback from inside particle

Summary: Fewer brown dwarfs with RF. Larger highest mass at given time. But similar **rates.**

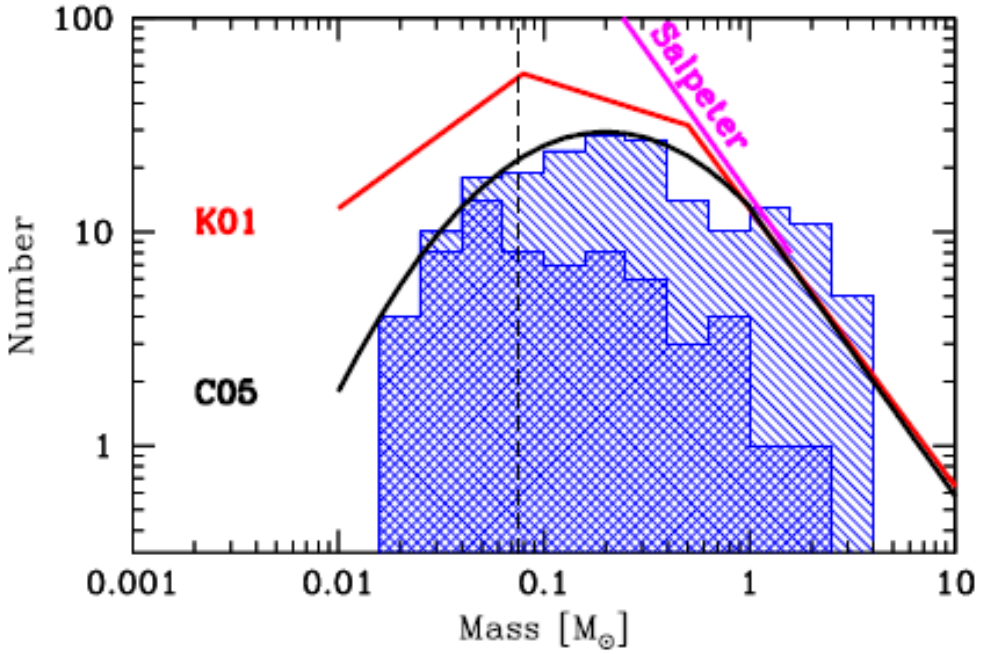

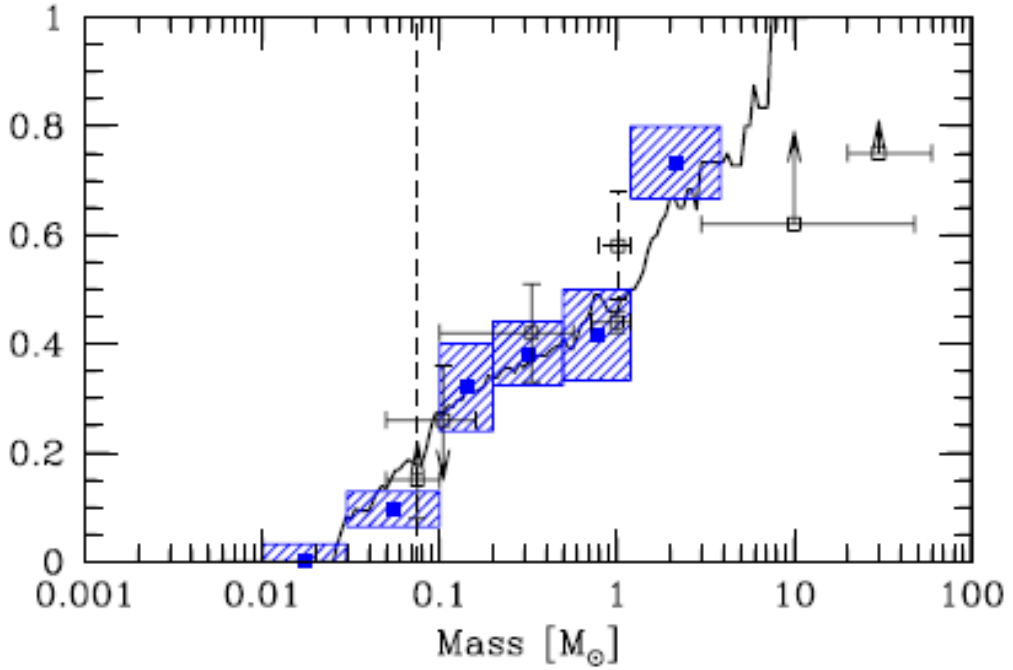

Conclusions

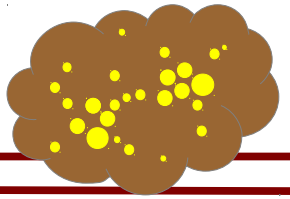

- Observations of the **IMF** suggest similar shapes but there are numerous mechanisms that **convert** the IMF into the **PDMF** as a function of time and environment.

- It is not sufficient to **reproduce** the IMF, **other observations** need to be reproduced as well.

- There seems to be a **connection** between the **IMF** and the **CMF** but further observations are needed to understand it.

- An analytic theory based on **Press-Schechter** is an interesting first approach to the problem, but does **not** take into account many of the **physical processes** that determine the shape of the IMF.

- Ultimately, we need **numerical simulations** to determine the shape of the IMF and its connection to the CMF. There are 2 main approaches: **AMR/SPH**. The results in both cases are significantly sensitive to **initial conditions.** The exploration of parameter space for the initial conditions is very costly. **Magnetic fields** are typically neglected, we expect them to lower SFR and increase outflows in simulations.

References

- Krumholz, Klein & McKee, 2012, ApJ, 754, 71
- Taylor and Miller, 2012, MNRAS, 426, 1687
- Bate, 2012, MNRAS, 419, 3115
- Bastian, Covey & Meyer, 2010, ARA&A, 48, 339
- Hennebelle & Chabrier, 2008, ApJ, 684, 395
- Bonnell, Larson & Zinnecker, 2007, Protostars & Planets V, B. Reipurth, D. Jewitt, and K. Keil (eds), University of Arizona Press, tucson, p.149-164
- Alves, Lombardi & Lada, 2007, A&A, 462, 17
- Lombardi, Alves & Lada, 2006, A&A, 454, 781
- Press & Schechter, 1974, 187, 425